

## Letter

# Development of superconducting joints between iron-based superconductor tapes

Yanchang Zhu<sup>1,3</sup>, Dongliang Wang<sup>1,2,4</sup> , Chundong Zhu<sup>3</sup>, He Huang<sup>1,2</sup> , Zhongtang Xu<sup>1,2</sup> , Shifa Liu<sup>1,2</sup>, Zhe Cheng<sup>1,2</sup> and Yanwei Ma<sup>1,2,4</sup> 

<sup>1</sup> Key Laboratory of Applied Superconductivity, Institute of Electrical Engineering, Chinese Academy of Sciences, Beijing 100190, People's Republic of China

<sup>2</sup> University of Chinese Academy of Sciences, Beijing 100049, People's Republic of China

<sup>3</sup> School of Materials Science and Engineering, Wuhan University of Technology, Wuhan 430070, People's Republic of China

E-mail: [dongliangwang@mail.iee.ac.cn](mailto:dongliangwang@mail.iee.ac.cn) and [ywma@mail.iee.ac.cn](mailto:ywma@mail.iee.ac.cn)

Received 5 February 2018, revised 16 April 2018

Accepted for publication 18 April 2018

Published 4 May 2018



## Abstract

Superconducting joints are essential for future iron-based superconductor applications. In this study, a process for fabricating superconducting joints between  $\text{Sr}_{1-x}\text{K}_x\text{Fe}_2\text{As}_2$  (Sr-122) tapes was developed for the first time. The Ag sheath was peeled off from one side of each sample. The exposed superconducting parts of the two tapes were joined and wrapped again with Ag foil. The diffusion bonding of the iron-based superconducting joint was achieved by the hot pressing (HP) process in an Ar atmosphere. The superconducting properties, microstructures, and elements distribution of the joint regions were investigated. The pressure was optimized in order to enhance the transport current of the joints. At 4.2 K and 10 T, a transport critical current  $I_c$  of 40 A for the joint was obtained, which was approximately 35.3% of the current capacity of the tapes themselves. Furthermore, the joint resistance was below  $10^{-9} \Omega$ . These results demonstrate that HP was useful for fabricating the superconducting joints.

Keywords: superconducting joint, iron-based superconductor, transport property, diffusion bonding, microstructures

(Some figures may appear in colour only in the online journal)

## 1. Introduction

Iron-based superconductors have become a major topic of discussion in recent years due to their unique performance, such as achieving high superconducting transition temperatures ( $T_c$ ) up to 55 K [1, 2], a large transport  $J_c$  over  $1 \text{ MA cm}^{-2}$  in thin films [3–5], and a high upper critical field above 100 T [6, 7] with low anisotropy ( $<2$  for Sr/BaKFeAs) [8, 9]. Significant progress toward high-performance iron-based conductors have been made over recent years [10–13]. For example, the  $J_c$  value of Ba-122 wire and tapes was rapidly improved to  $1.5 \times 10^5 \text{ A cm}^{-2}$  at 4.2 K and 10 T in short

samples [14], and the 100 m class  $\text{Sr}_{1-x}\text{K}_x\text{Fe}_2\text{As}_2$  (Sr-122) tapes were fabricated last year [15]. However, for large-scale use, it is very common to connect several pieces of long iron-based superconducting tapes. Hence, a superconducting joint is very important for lowering the total heating generation, and for persistent current operation. In order to operate the magnet in the persistent mode, the joints between the coils must be superconducting even under a high magnetic field. Therefore, the joints between two superconducting wires or tapes have become one of the most important technologies.

So far, techniques for joining superconductor wires/tapes such as NbTi, BiSCCO, and  $\text{MgB}_2$  wires/tapes have been well developed [16–25]. For the low temperature superconductors, especially for NbTi, joining methods are very

<sup>4</sup> Authors to whom correspondence should be addressed.

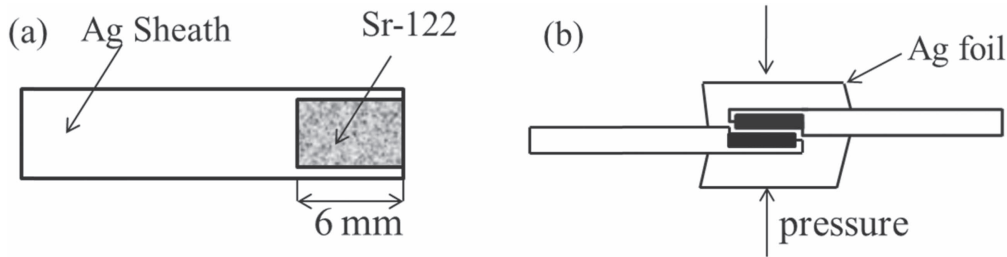


**Figure 1.** Schematic of the joining process: (a) peeling off the sheath metal; (b) wrapping in Ag foil.

mature and convenient for the manufacture of persistent mode magnets. Soldering with solder alloy is one choice in commercial magnet manufacturing, and the critical current of the joints can reach as high as 1000 A at 4.2 K and 1 T [20], with resistance in the range of  $10^{-13} \sim 10^{-14} \Omega$ . Cold pressing is another good choice to connect the NbTi filaments [21, 22]. The current of joints fabricated by this method was as high as 468 A (1 T, 4.2 K). Persistent  $\text{MgB}_2$  joints have been made predominantly by powder in tube (PIT) techniques, which are similar to those used in wire production. The critical current ratio (CCR) value can reach 90% at 4.2 K, and the joint resistance reaches  $10^{-10} \sim 10^{-12} \Omega$  [17]. Oomen [23] used the hot pressing (HP) technique at slightly lower temperatures between 600 and 700 °C to fabricate joints with dense and well-connected filler materials. CCR values for these joints were only 25 ~ 50% at 4.2 K and 1 T, and the resistance was below  $10^{-9} \Omega$ . The formation of joints between BiSCCO is typically fabricated by repeating the heat treatment process used for the conductor itself. This involves cold pressing of the exposed filaments of particularly reactive tapes followed by the same extensive thermomechanical treatment used to form the BiSCCO phase in the conductor [24, 25]. The critical current of the joints could be higher than in the tapes, as reported by Chen *et al* [16], and the joint resistance was estimated to be below  $10^{-12} \Omega$  at 4.2 K and self-field. In addition, a ground-breaking demonstration was made in the joint methods of REBCO-coated conductors [26, 27]. Park *et al* [26] prepared a well-bonded lap joint by partial melting of the REBCO layers under low  $\text{PO}_2$ . The critical current (84 A) of the joint at 77 K and self-field was achieved, and a joint resistance less than  $10^{-17} \Omega$  was confirmed by using a decay measurement at 77 K and self-field [26].

Until now, joining iron-based superconducting tapes has not been reported, and the joining method for these tapes is much more difficult than for others. Firstly, like cuprate superconductors, iron-based superconducting cores are more fragile and harder than the sheath materials. Thus, it is very difficult to join two pieces of iron-based superconductor composite tape simply by cold pressing, like in NbTi's case. On the other hand, the iron-based superconductor is sensitive to the air during reaction temperatures [28], which means that the sintering process must be made in inert atmosphere. In general, the lap joint method and diffusion bonding, which show good joint properties between cuprate superconductors, can be adopted for iron-based superconductors. Besides, it was found that the HP process could significantly increase the transport  $J_c$  of Sr-122 tape by improving the core density

**Table 1.** Parameters of the HP process.

Samples	HP50	HP100	HP200	HP300
Pressure (MPa)	2.3	4.6	9.2	13.8
Pressing time (h)	0.5	0.5	0.5	0.5

and grain alignment simultaneously [12]. Recently, a transport  $J_c$  value up to  $0.15 \text{ MA cm}^{-2}$  at 4.2 K and 10 T was obtained in Ba-122 tapes through the HP method [14]. According to these results [12, 14], it is possible to form Sr-122 joints between two pieces of Sr-122 tapes by using the HP method; during this process the Sr-122 grains of the connecting area heal better, and connect.

In this paper, a method of joining Sr-122 tapes using HP was first proposed. Samples of single filament Sr-122 tapes were joined by this process. The critical current  $I_c$  and the joint resistance of samples were measured at 4.2 K and in different magnetic fields. The  $I_c$  was 40 A at 4.2 K and 10 T; meanwhile, the joint resistance estimated from the  $I$ - $V$  curve was below  $10^{-9} \Omega$ .

## 2. Experimental details

The Sr-122 tapes were fabricated by the *ex situ* PIT method. Firstly, Sr fillings, K pieces, and Fe and As powders were mixed by the ball-milling method. The mixed powders were loaded into Nb tubes, and then sintered at 900 °C for 35 h. The sintered superconducting bulk was ground into powders under Ar atmosphere, and then the Sn material was added to increase grain connectivity. The fine powders were finally packed into Ag tubes with an 8 mm outer diameter and a 5 mm inner diameter. These tubes with a mono-core inside were finally deformed into tapes with thicknesses of 0.4 mm. Finally, short samples were cut from the long tapes, and then sintered at 880 °C for 0.5 h in Ar atmosphere.

Figure 1 shows a schematic view of the assembly method. The sides of the sheath materials were partially peeled off mechanically. The width of the joints was 3.5 mm, and the wrap length was 6 mm. No additional bonding agent was used. The joints were heat-treated in Ar atmosphere, and the thermal cycle was the same as in the heat treatment process for the unjoined tapes. We conducted a series of controlled experiments to investigate the effect of pressure on the joint properties. The parameters of the HP process are shown in table 1.

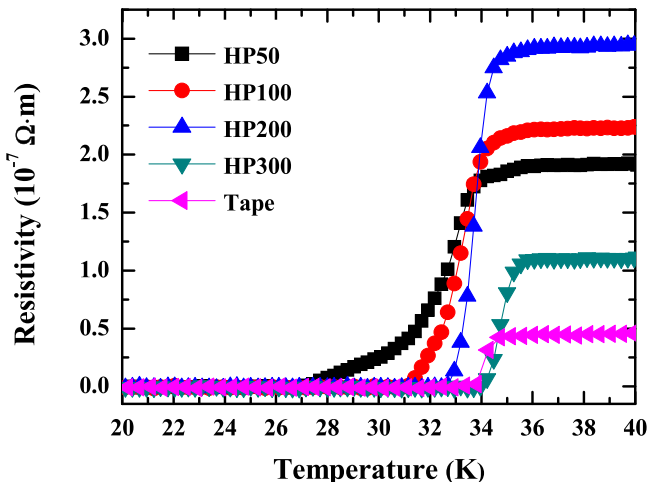


**Figure 2.** Temperature dependence of resistivity for the unjoined tape and joints.

We used x-ray computed tomography (XCT; GE Micromex) to analyze the crack distribution of the connection area of the joints. Microstructures in the joint area were observed by electron probe microanalysis (EPMA; JEOL JXA8230). The temperature dependence of the resistivity at 0 T was determined using a four-probe method by a physical property measurement system (model: PPMS-9). Transport critical currents ( $I_c$ ) of the samples were measured at 4.2 K using a standard four-probe technique, with a criterion of  $1 \mu\text{V cm}^{-1}$ . The magnetic field dependence of transport  $I_c$  values for all samples were evaluated at the High Field Laboratory for Superconducting Materials in Sendai, or at the Institute of Plasma Physics, CAS in Hefei.

### 3. Results and discussions

As shown in figure 2, the temperature dependence of the resistance at self-field for all samples was measured using a typical standard four-probe method at 4.2 K. Table 2 lists the  $T_c^{\text{onset}}$ ,  $T_c^{\text{zero}}$ , and transition width of all samples. We can see from the curves that samples HP300 and HP200 show a sharp transition compared to HP50 and HP100. The  $T_c^{\text{zero}}$  values of the joints are increased as the pressure increases, suggesting that the impurity phase formed in the connection area significantly affects the superconducting transition of the joints. Furthermore, the smaller transition width  $\Delta T_c$  of 1.2 K and 1 K obtained for samples HP200 and HP300 are very close to those of the tapes; meanwhile, those of HP50 and HP100 are 2.4 K and 2.3 K, respectively. These results suggest that the superconducting phases of HP300 and HP200 are more homogeneous.

In order to further characterize the samples' properties, we tested their critical currents. The voltage and current terminals were attached on either side of the joint to measure the voltage of the joined sample. The distance between the voltage terminals was 20 mm for all samples. As an example, the voltage of HP200 at 4.2 K and 10 T is plotted in figure 3(a). The calculated transport  $I_c$  of HP200 was 40 A at

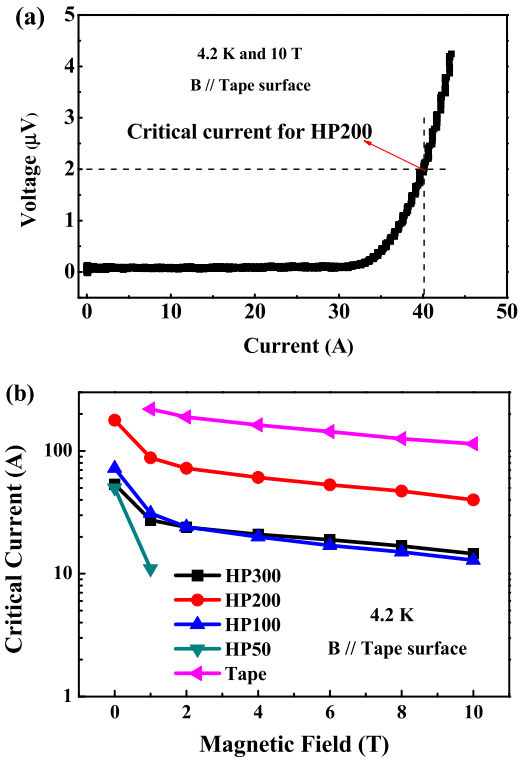


**Figure 3.** (a)  $I$ - $V$  characteristics of the joint for HP200 measured at 4.2 K and 10 T. (b) Magnetic field dependence of transport critical current at 4.2 K for joints and unjoined tape.

**Table 2.** Transition width of the joints and unjoined tape.

Samples	$T_c^{\text{onset}}$ (K)	$T_c^{\text{zero}}$ (K)	$\Delta T_c$ (K)
HP50	32.7	30.39	2.4
HP100	33.99	31.69	2.3
HP200	34.65	33.45	1.2
HP300	35.5	34.5	1
Tape	34.57	33.84	0.7

4.2 K and 10 T, with a criterion of  $1 \mu\text{V cm}^{-1}$ . The joint resistances  $dV/dI$  estimated from the  $I$ - $V$  curve were below  $10^{-9} \Omega$ . However, the accuracy of this  $I$ - $V$  measurement system was  $10^{-9} \Omega$ , and thus accurate resistance data should be measured by using the inductive method, which was not mentioned in this work. Figure 3(b) presents the magnetic field dependence of transport  $I_c$  at 4.2 K for the Sr-122 joint tapes hot-pressed at different pressures. The applied fields up to 10 T were parallel to the joint surface. The critical current of sample HP50 was too low to be measured in the magnetic field over 2 T. As evident from the figure,  $I_c$  increased monotonically with the increase of HP pressure load up to 9.2 MPa, and then rapidly decreased with further increasing pressure load to 13.8 MPa. The best Sr-122 joint HP200 exhibited a CCR ( $\text{CCR} = I_c^{\text{joint}}/I_c^{\text{unjoined}}$ ) of 35.3% at 10 T and 4.2 K; this is the first time that such results have been reported for iron-based tapes. Besides, a superconducting current as high as 178 A was achieved at 4.2 K and self-field, and the CCR of samples HP100 and HP300 were 11.3% and 12.8% at 4.2 K and 10 T, respectively. To understand the

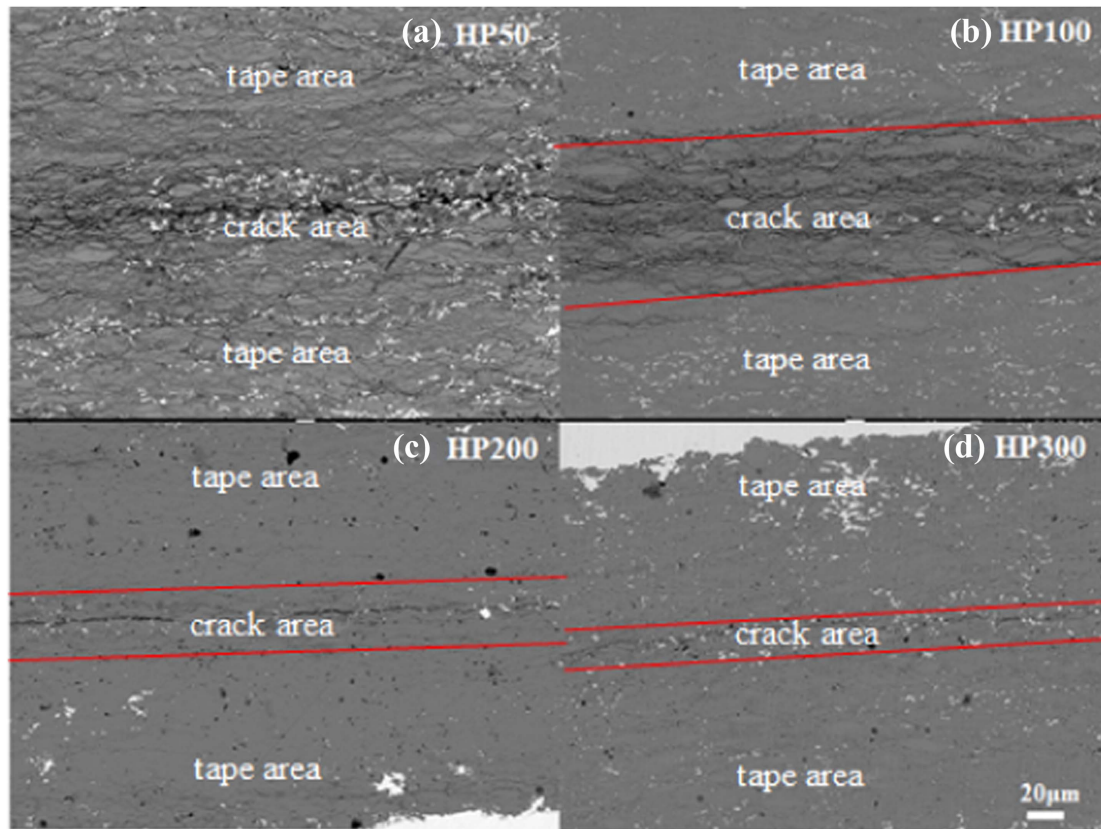


**Figure 4.** SEM images of longitudinal cross sections of Sr-122 superconducting joints.

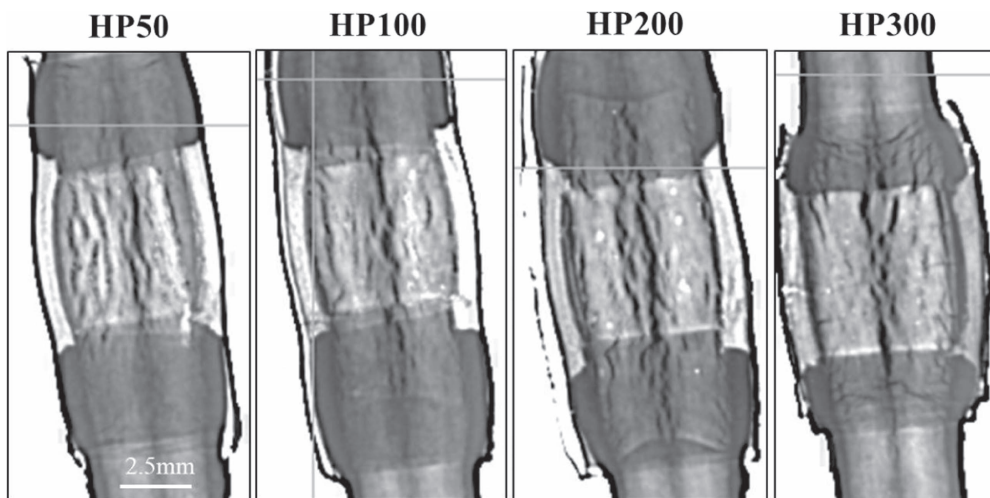


**Figure 5.** XCT images of the joints.

complex effects of pressure on transport performance, the microstructure of the joints were analyzed.

SEM images of longitudinal cross sections of the joints under different pressure values are shown in figure 4. There are many micro-cracks in the whole cross section (figure 4(a)). In figure 4(b) the micro-cracks in the tape area decrease, and are mainly concentrated in the joint region. When the pressure further increases to 13.8 MPa, there are almost no obvious micro-cracks in the tape area. Meanwhile, as the pressure increases, the number of micro-cracks around the connection

area decreases. This indicates that the micro-cracks in the whole joint section significantly decrease with increasing pressure. Thus, as the pressure increases, the tapes are well assembled, and may load a large transport current. However, the reason that the transport properties of sample HP300 are less than those of HP200 needs to be analyzed further.

Figure 5 shows the XCT images of joints HP50, HP100, HP200, and HP300. All the samples have longitudinal macro-cracks along the direction of current transport, and the longitudinal macro-cracks decrease with increasing pressure.



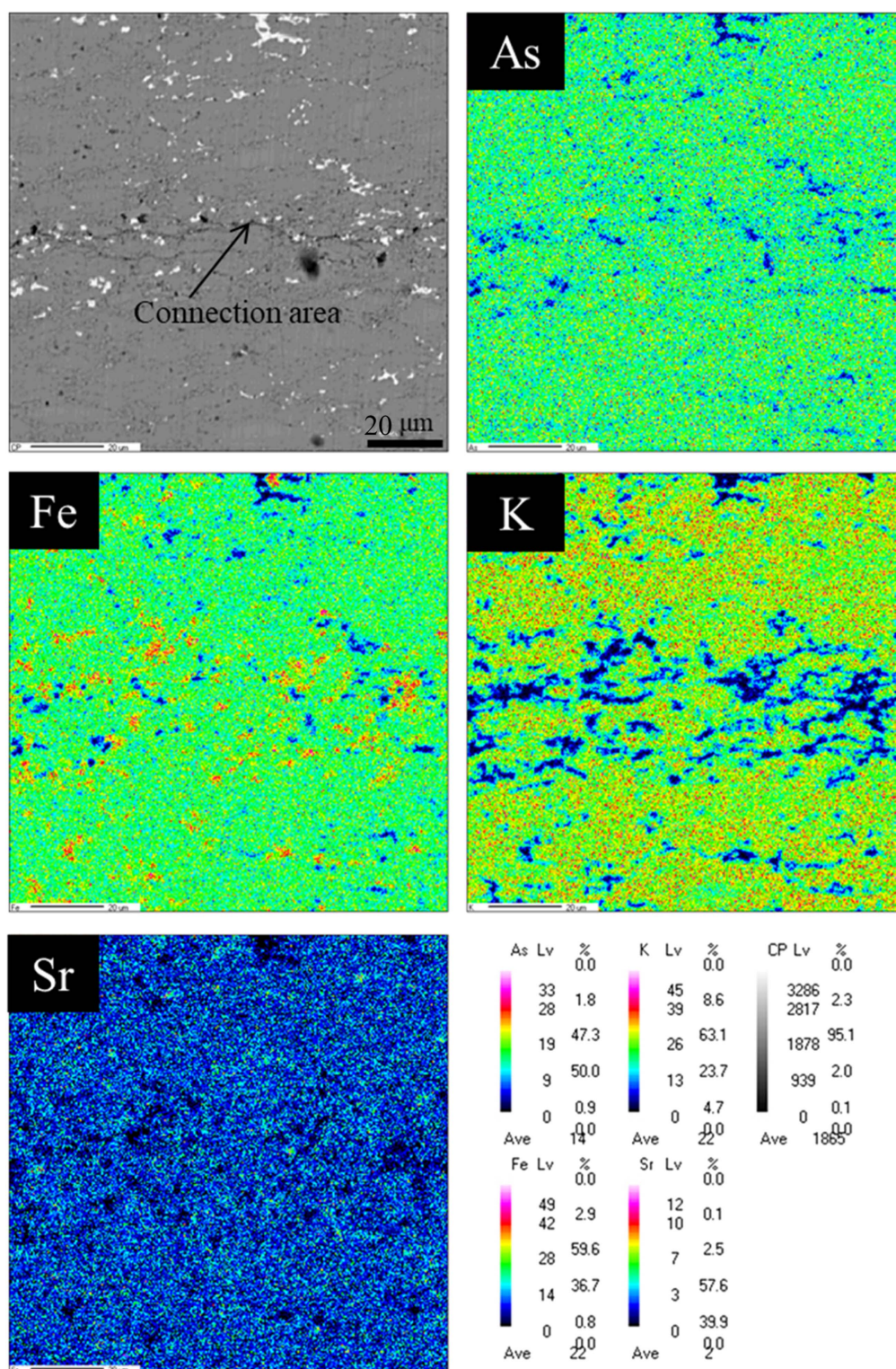


**Figure 6.** SEM and EPMA mapping images of the joint HP300.

At the same time, transverse macro-cracks occur when the pressure increases to 13.8 MPa. These results indubitably indicate that all the cracks are harmful to the transport performance of the joints, but the effect of transverse macro-cracks on blocking the current is larger than that of longitudinal macro-cracks. This may be the main reason why the critical currents of joints are not improved continuously with

increasing pressure. Although sample HP300 shows a more homogeneous superconducting phase and less longitudinal cracks in the connection area than other samples, the CCR of sample HP200 is larger than that of HP300 when the applied pressure is 9.2 MPa.

To characterize the microstructure of the joint more adequately, EPMA mapping images are shown in figure 6,

which further demonstrates the element distribution of sample HP300. Elements Sr, K, Fe, and As of the superconducting phase are almost homogeneously distributed in the tape area. However, K is deficient around the connection area, especially along the crack, which can also explain the low superconducting performance of the joint compared to unjoined tapes.

According to the results shown above, it is clear that the transport properties of iron-based superconducting joints are affected mainly by the superconducting phases and microstructures in the connection area. Firstly, in this work, three kinds of cracks are observed: longitudinal macro-cracks, transverse macro-cracks, and micro-cracks. Transverse macro-cracks are more harmful to the transport performances of tapes compared to the longitudinal ones. Meanwhile, micro-cracks will block the current transport from one tape to another tape. Therefore, these cracks should be avoided in the joint section. Secondly, the K loss in the joint area should also be avoided because the more K loss there is, the more impurities there are. The loss of K usually happens at high temperature, and thus, extending the pressing time could eliminate this problem. Thirdly, the texture degree in the connection area is also very important, although not mentioned in this work. It is well-known that *c*-axis texture should be induced to relieve the weak-link effect at grain boundaries for iron-based superconducting samples. However, in our case, the crack problem should be resolved firstly before achieving a high texture degree in the connection area. A bonding agent could be useful for eliminating cracks in joints. In the future, further increase of the transport current for the joint is expected by tailoring diffusion bonding parameters and bonding agents.

#### 4. Conclusion





In summary, we successfully fabricated the world's first joint of iron-based Sr-122 tapes with a resistance  $<10^{-9}\Omega$ . The joints were hot-pressed under various pressures of 2.3 MPa  $\sim$  13.8 MPa and a pressing time of 0.5 h. It is found that the pressure significantly affects the CCR of the joints. Our results show that the optimized pressure parameters are suitable for assembling two superconducting cores. The highest CCR of 35.3% (at 4.2 K in 10 T) is obtained for the Sr-122 joint pressed at 9.2 MPa with a pressing time of 0.5 h. Besides, a superconducting current as high as 178 A is achieved at 4.2 K and self-field.

#### Acknowledgments

The authors would like to thank Professor S Awaji at Sendai, and Dr Fang Liu, Mr Lei Lei, and Professor Huajun Liu at Hefei for  $I_c$ -*B* measurement. This work is partially supported by the National Natural Science Foundation of China (Grant No. 51577182 and 51320105015), the Beijing Municipal Science and Technology Commission (Grant No. Z171100002017006),

the Bureau of Frontier Sciences and Education, Chinese Academy of Sciences (QYZDJ-SSW-JSC026), and the Key Research Program of the Chinese Academy of Sciences (Grant No. XDPB01-02).

#### ORCID iDs

Dongliang Wang  <https://orcid.org/0000-0001-7052-4182>  
 He Huang  <https://orcid.org/0000-0002-8482-3682>  
 Zhongtang Xu  <https://orcid.org/0000-0002-1812-3362>  
 Yanwei Ma  <https://orcid.org/0000-0002-7131-0888>

#### References

- [1] Rotter M, Tegel M and Johrendt D 2008 *Phys. Rev. Lett.* **101** 107006
- [2] Ma Y W 2015 *Physica C* **516** 17
- [3] Katase T, Ishimaru Y, Tsukamoto A, Hiramatsu H, Kamiya T, Tanabe K and Hosono H 2010 *Supercond. Sci. Technol.* **23** 082001
- [4] Lee S *et al* 2010 *Nat. Mater.* **9** 397
- [5] Katase T, Hiramatsu H, Kamiya T and Hosono H 2010 *Appl. Phys. Express* **3** 063101
- [6] Ni N, Bud'ko S L, Kreyssig A, Nandi S, Rustan G E, Goldman A I, Gupta S, Corbett J D, Kracher A and Canfield P C 2008 *Phys. Rev. B* **78** 014507
- [7] Wang X L *et al* 2010 *Phys. Rev. B* **82** 024525
- [8] Yamamoto A *et al* 2009 *Appl. Phys. Lett.* **94** 062511
- [9] Yuan H Q, Singleton J, Balakirev F F, Baily S A, Chen G F, Luo J L and Wang N L 2009 *Nature* **457** 565
- [10] Gao Z S, Ma Y W, Yao C, Zhang X P, Wang C L, Wang D L, Awaji S and Watanabe K 2012 *Sci. Rep.* **2** 998
- [11] Lin H, Yao C, Zhang X, Zhang H, Zhang Q, Wang D and Ma Y 2013 *Physica C* **490** 37
- [12] Lin H *et al* 2014 *Sci. Rep.* **4** 6944
- [13] Yao C, Lin H, Zhang X P, Wang D L, Zhang Q J, Ma Y W, Awaji S and Watanabe K 2013 *Supercond. Sci. Technol.* **26** 075003
- [14] Huang H, Yao C, Dong C H, Zhang X P, Wang D L, Cheng Z, Li J Q, Satoshi A, Wen H H and Ma Y W 2018 *Supercond. Sci. Technol.* **31** 015016
- [15] Zhang X, Oguro H, Yao C, Dong C, Xu Z, Wang D, Awaji S, Watanabe K and Ma Y 2017 *IEEE Trans. Appl. Supercond.* **27** 7300705
- [16] Chen P, Trociewitz U P, Davis D S, Bosque E S, Hilton D K, Kim Y, Abrahimov D V, Starch W L, Jiang J and Hellstrom E E 2017 *Supercond. Sci. Technol.* **30** 025020
- [17] Li X H, Ye L Y, Jin M J, Du X J, Gao Z S, Zhang Z C, Kong L Q, Yang X L, Xiao L Y and Ma Y W 2008 *Supercond. Sci. Technol.* **21** 025017
- [18] Patel D, Al Hossain M S, Maeda M, Shahabuddin M, Yanmaz E, Pradhan S, Tomsic M, Choi S and Kim J H 2016 *Supercond. Sci. Technol.* **29** 095001
- [19] Takayasu M 1999 *IEEE Trans. Appl. Supercond.* **9** 4628
- [20] Liu S Y, Jiang X H, Chai G L and Chen J B 2013 *IEEE Trans. Appl. Supercond.* **23** 4400504
- [21] Tominaka T, Kakugawa S, Hara N and Maki N 1991 *IEEE Trans. Magn.* **27** 1846
- [22] Wen H M, Lin L Z and Han S 1992 *IEEE Trans. Magn. Supercond.* **28** 834
- [23] Oomen M P 2014 *Applied Superconductivity Conf. (Charlotte, NC, USA)*

- [24] Lee H G, Hong G W, Kim J J and Song M Y 1995 *Physica C* **242** 81
- [25] Iyer A N, Lu W, Mironova M, Vipulanandan C, Balachandran U and Salama K 2000 *Supercond. Sci. Technol.* **13** 187
- [26] Park Y J, Lee M W, Oh Y K and Lee H G 2014 *Supercond. Sci. Technol.* **27** 085008
- [27] Brittles G D, Mousavi T, Grovenor C R M, Aksoy C and Speller S C 2015 *Supercond. Sci. Technol.* **28** 093001
- [28] Sefat A S 2013 *Curr. Opin. Solid State Mater. Sci.* **17** 59–64